Gravity-driven film flow with variable physical properties

Helge I. Andersson
Department of Energy and Process Engineering, The Norwegian University of Science and Technology, 7491 Trondheim, Norway

Bidyut Santra
Department of Mathematics, Jangipur College, Mushidabad 742213, India

Bhabani S. Dandapat
Physics and Applied Mathematics Unit, Indian Statistical Institute, 203 B.T. Road, Calcutta 700 108, India

(Received 23 February 2006; accepted 28 June 2006; published online 8 August 2006)

The laminar flow and heat transfer in an accelerating thin liquid film are considered with the view to examine the influence of variable density and transport properties. A new similarity transformation is proposed which exactly transforms the hydrodynamic and thermal boundary layer equations for vertically falling film flow into a coupled set of ordinary differential equations. The resulting two-point boundary value problem is integrated numerically with empirical data for the physical properties of water. For given inflow conditions, the temperature-dependency of the dynamic fluid viscosity makes both the hydrodynamic and thermal boundary layers thinner with increasing wall temperature. The expected thickening of the thermal boundary layer due to the increasing thermal diffusivity is therefore more than outweighed by the decreasing viscosity. The nonlinear variation of the physical properties makes these effects more pronounced at the lower inflow temperature.

I. INTRODUCTION

Falling films are frequently encountered in the process industry, e.g., in evaporators and condensers and for heating or cooling purposes in chemical and nuclear reactors. The hydrodynamics of gravity-driven liquid films and the accompanying heat and mass transfer have been extensively studied over the years. A prevailing assumption in the vast majority of these investigations is the constancy of the physical properties of the liquid. However, half a century ago Voskresensky[1] accounted for the temperature-dependency of the physical properties of a condensate film. Somewhat later Poots and Miles[2] concluded that the discrepancy between their analysis and the classical Nusselt theory was due to the neglect of the nonlinear effects of variable condensate properties and vapor drag in the latter simplistic approach. They furthermore found that the effect of variable fluid properties became negligible for Prandtl numbers above 1. More recently, an extended study of laminar film condensation of superheated vapor was presented by Shang and Wang.[3] Their analysis used the same empirical expressions for the density, dynamic viscosity, and thermal conductivity as in the preceding study by Shang *et al.*[4] of laminar free convection of water with variable thermophysical properties.

The purpose of the present study is to examine the influence of variable physical properties on the gravity-driven laminar flow of a thin liquid film falling along a vertical wall. The momentum and thermal (or mass) boundary layer problem for a constant-property film was solved by Andersson.[5] By means of a Falkner-Skan-type of transformation, exact similarity solutions for the velocity and temperature fields were provided. Thereafter, Andersson *et al.*[6] adopted the Boussinesq approximation as a first approach to account for temperature variations of the physical properties of the falling liquid film, i.e., by allowing a *linear* variation of the density with temperature in the body force term in the hydrodynamic boundary layer equation. With the same similarity transformation as in Ref. 5 the governing equations were transformed to a set of ODEs. The presence of a buoyancy term in the transformed momentum equation facilitated investigations of both favorable (aiding) and unfavorable (opposing) buoyancy on the hydrodynamics and heat transfer.

In the present paper not only the density but also the viscosity and thermal conductivity will be allowed to vary with the temperature. A Falkner-Skan-type of transformation is therefore no longer applicable and a new similarity transformation is required. Thereafter, the resulting set of ODEs will be solved numerically. To demonstrate the effect of variable physical properties on the flow and heat transfer, *nonlinear* empirical temperature correlations for water are used. Results for a film with inflow temperature 20 °C will be presented and compared with results for a film at 60 °C.

II. PHYSICAL MODEL AND MATHEMATICAL FORMULATION

Let us consider the accelerating flow of a thin liquid film down along a vertical wall, as depicted in Fig. 1. The film Reynolds number is sufficiently low so that the flow remains laminar and the free surface is free of waves. Uniform flow enters the system at $x=0$ with a constant temperature T_0 and falls vertically down along the smooth wall which is kept at a constant temperature T_w. A hydrodynamic and a thermal boundary layer with thicknesses $\delta(x)$ and $\delta_T(x)$ develop

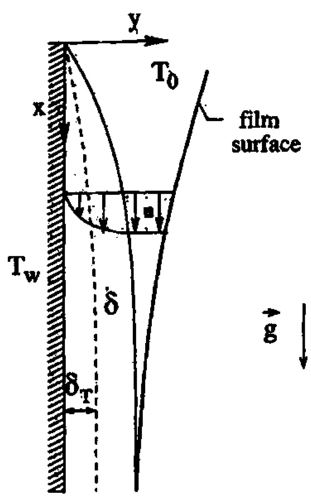

FIG. 1. Schematic representation of gravity-driven film flow and coordinate system.

along the wall. The flow outside the hydrodynamic boundary layer remains quasi-one-dimensional and is governed by the inviscid equation of motion

$$\rho U dU/dx = \rho g, \tag{1}$$

where g is the gravitational acceleration. With zero velocity and infinite film thickness at the inlet $x=0$, Eq. (1) is readily integrated once to give

$$U(x) = (2gx)^{1/2} \tag{2}$$

This particular form of the inviscid flow solution belongs to the classical Falkner-Skan-type[7] of free-streams $U(x) \sim x^m$ for flow along wedge-shaped bodies with included wedge angle $2\pi m/(m+1)$. The part of the liquid film outside the thermal boundary layer is unaffected by the heat transfer between the vertical wall and the fluid and therefore remains isothermal with temperature T_0.

The velocity and temperature inside the hydrodynamic and thermal boundary layers are governed by the conservation equations for mass, momentum and thermal energy

$$\frac{\partial}{\partial x}(\rho u) + \frac{\partial}{\partial y}(\rho v) = 0, \tag{3}$$

$$\rho\left(u\frac{\partial u}{\partial x} + v\frac{\partial u}{\partial y}\right) = \rho g + \frac{\partial}{\partial y}\left(\mu\frac{\partial u}{\partial y}\right), \tag{4}$$

$$\rho C_p\left(u\frac{\partial T}{\partial x} + v\frac{\partial T}{\partial y}\right) = \frac{\partial}{\partial y}\left(\kappa\frac{\partial T}{\partial y}\right) \tag{5}$$

with boundary conditions

$$u = v = 0, T = T_w \quad \text{at } y = 0 \tag{6a}$$

$$u(x,y) \to U(x) \quad \text{as } y \to \delta(x) \tag{6b}$$

$$T(x,y) \to T_0 \quad \text{as } y \to \delta_T(x). \tag{6c}$$

Streamwise diffusion of streamwise momentum and heat have been neglected in (4) and (5) in accordance with aerodynamic boundary layer theory. The coupled problem defined by Eqs. (3)–(6) is identical to a compressible boundary layer problem, except that heat generation by viscous dissipation $\mu(\partial u/\partial y)^2$ is assumed to be negligible and the $u\partial p/\partial x$ term is absent in (5) since the present fluid is incompressible by nature. In the hydrodynamic context, this system has three dependent variables: u, v, and T. To render the boundary value problem (BVP) determinate, however, the temperature variation of the film density ρ, the dynamic viscosity μ, the thermal conductivity κ, and the specific heat C_p must be known. The special case with constant physical properties simplifies to the problem considered by Andersson.[5] In that work, a Falkner-Skan-type of similarity transformation was devised which exactly transformed the governing PDEs into a set of ODEs.

III. SIMILARITY TRANSFORMATION AND SOLUTION PROCEDURE

In the present study where we aim to investigate the influence of variable physical properties (ρ, μ, κ, and C_p), we devise a new similarity transformation inspired by the Howarth-Dorodnitsyn transformation in compressible boundary layer theory, see e.g., Schreier.[8] Let us first define a stream function $\psi(x,y)$:

$$\rho u = \frac{\partial \Psi}{\partial y}; \quad -\rho v = \frac{\partial \Psi}{\partial x} \tag{7}$$

such that mass conservation (3) is automatically satisfied. The similarity variable η and the new dependent variables f and Θ are defined as:

$$\eta = \left(\frac{3U}{4\nu_0 x}\right)^{1/2} \int_0^y (\rho/\rho_0)dy, \tag{8}$$

$$\Psi(x,y) = \rho_0\left(\frac{4U\nu_0 x}{3}\right)^{1/2} \cdot f(\eta), \tag{9}$$

$$\Theta(\eta) = \frac{T(x,y) - T_0}{T_w - T_0}, \tag{10}$$

where $U=U(x)$ is given by (2). Here, ρ_0, μ_0, κ_0, and C_{p0} are the values of the fluid properties of the incoming liquid at $x=0$, i.e., at temperature T_0, and $\nu_0 \equiv \mu_0/\rho_0$ is the corresponding kinematic viscosity. It should be emphasized that the transformation (10) exists only if $T_w \neq T_o$. In the special case $T_w = T_o$, however, the trivial solution $T(x,y) = T_o$ solves the thermal energy Eq. (5) subject to the boundary conditions (6a) and (6c) and no similarity transformation is needed.

The coupled boundary layer problem (3)–(6) now transforms into the following BVP:

$$\left[\frac{\rho\mu}{\rho_0\mu_0} f''\right]' + ff'' + \frac{2}{3}(1 - f'^2) = 0, \tag{11}$$

$$\left(\frac{\rho\kappa}{\rho_0\kappa_0}\Theta'\right)' + \frac{C_p}{C_{po}} \cdot \mathrm{Pr}_0 \cdot f\Theta' = 0, \tag{12}$$

$$f = f' = 0 \quad \text{and } \Theta = 1 \quad \text{at } \eta = 0, \tag{13a}$$

TABLE I. Local Nusselt number Nu_x for film flow with constant fluid properties.

Pr	$Nu_x Re_x^{-1/2}$	
	Present	Andersson (Ref. 5)
0.03	0.10910309	0.109103
0.06	0.14923170	0.149231
0.10	0.18682623	0.186825
0.30	0.29686354	0.296863
0.60	0.39184572	0.391845
1.00	0.47757197	0.477572
3.0	0.71927337	0.719274
6.0	0.92341665	0.923417
10.0	1.10671261	1.10671
30.0	1.62338539	1.62339

$$f' \to 1 \quad \text{and}\ \Theta \to 0 \quad \text{as}\ \eta \to \infty, \tag{13b}$$

where $Pr_0 \equiv \mu_0 C_{p0}/\kappa_0$ is the constant Prandtl number of the isothermal inflow.

The ODE (11) governing the flow in the hydrodynamic boundary layer is coupled to the thermal boundary equation (12) via the temperature-dependent density and viscosity. In the particular case with constant fluid properties, this coupling vanishes and both the similarity transformation (8)–(10) and the resulting BVP (11)–(13) degenerate to that considered by Andersson.[5]

A criterion for exact similarity to exist is that all coefficients in (11) and (12) are either constants or functions of η only. In the following section, empirical temperature correlations will be given for the fluid properties; i.e., $\rho(T)$, $\mu(T)$, $\kappa(T)$, and $C_p(T)$. Since the temperature T is uniquely related to the dimensionless temperature $\Theta(\eta)$, i.e., $T(x,y)=T_0+\Theta(\eta)\cdot(T_w-T_0)$ according to Eq. (10), the requirements for similarity are fulfilled in the present context. In compressible boundary layer theory, however, the so-called Chapman-Rubesin parameter $(\rho\mu/\rho_0\mu_0)$ in Eq. (11) is often taken as a constant to assure similarity.

The nonlinear two-point boundary value problem (11)–(13) defined on the semi-infinite interval $\eta\in[0,\infty)$ is first formulated as a set of five first-order ODEs and thereafter integrated as an initial value problem over the finite interval $\eta\in[0,\eta_\infty]$, whereas five corresponding adjoint equations (adjunct to analytically determined variational equations) are subjected to backward integration. Particular attention is paid to assure that η_∞ is sufficiently large. The accuracy of the adopted integration procedure can be verified by comparisons with the results in Ref. 5 for constant fluid properties, see Table I.

IV. EMPIRICAL CORRELATIONS FOR THE PHYSICAL PROPERTIES

In order to solve the transformed boundary layer problem for a particular fluid, the variation with temperature of the physical properties is required. Here, we consider water at atmospheric pressure and adopt the empirical correlations suggested by Shang *et al.*:[4]

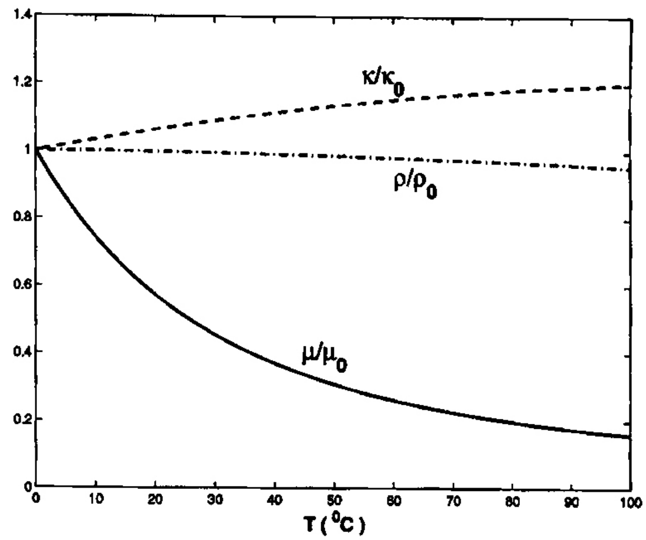

FIG. 2. Temperature variations of density ρ, dynamic viscosity μ, and thermal conductivity κ for water at atmospheric pressure. According to the empirical correlations (14)–(16) adopted from Shang *et al.* (Ref. 3). Here, each property has been normalized with its value at 0 °C; i.e., $\rho_0=999.8\ \mathrm{kg\,m^{-3}}$, $\mu_0=1.787\cdot10^{-3}\ \mathrm{kg\,m^{-1}\,s^{-1}}$, $\kappa_0=0.563\ \mathrm{W\,m^{-1}\,K^{-1}}$.

$$\rho(T)=[-4.88\times10^{-3}K^{-2}(T-273K)^2+999.9]\ \mathrm{kg\,m^{-3}}, \tag{14}$$

$$\mu(T)=\exp[-1.6-1150K\cdot T^{-1}+(690K\cdot T^{-1})^2]\times10^{-3}\ \mathrm{kg\,m^{-1}\,s^{-1}}, \tag{15}$$

$$\kappa(T)=[-8.01\times10^{-6}K^{-2}(T-273K)^2+1.94\times10^{-3}K^{-1}(T-273K)+0.563]\ \mathrm{W\,m^{-1}\,K^{-1}}. \tag{16}$$

Here, T is taken as the absolute temperature in Kelvin. The correlations (14) and (16) were deduced by Shang *et al.*[4] on the basis of experimental data[9] for water over the temperature range 0–100 °C. The deviation of (14) and (16) from the experimental data was reported to be within 0.35% and 0.18%, respectively. The viscosity correlation (15) for water used by Shang *et al.*[4] was taken from Chang[10] and compared with experimental data[9] to within 1.8%. The variation of ρ, μ, and κ with temperature according to Eqs. (14)–(16) is shown in Fig. 2. It is readily seen that the relative variation of the density is practically negligible compared to the significant variations of the thermal conductivity and, in particular, of the viscosity. It is well known that the specific heat capacity C_p is practically independent of the temperature for most liquids. For water, as considered herein, the variation of C_p over the temperature range 0–100 °C is less than 1%. We therefore take $C_p=C_{p0}=4.20\cdot10^3\ \mathrm{J\,kg^{-1}\,K^{-1}}$ in accordance with Shang *et al.*[4] An immediate implication of the above assumptions is that the Prandtl number $Pr\equiv\mu C_p/\kappa$ varies from about 13 at 0 °C to ≈1.76 at 100 °C, i.e., a reduction by a factor of about 7. This substantial decrease of Pr with T is primarily due to the reduction of μ but also due to the 20% increase of κ from 0 °C to 100 °C.

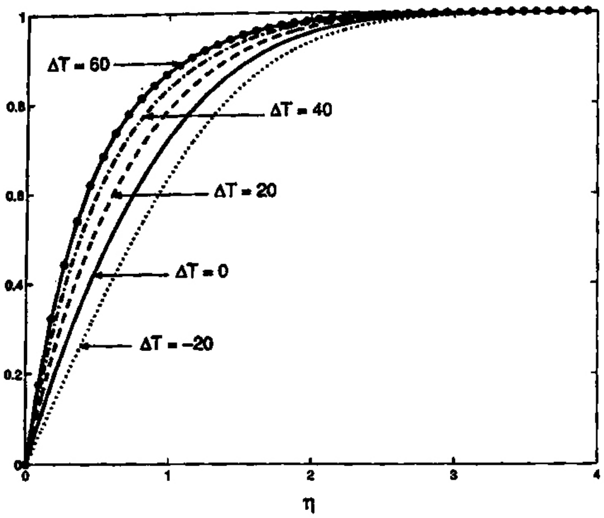

FIG. 3. Characteristic velocity profiles $f'(\eta)$ for some different ΔT (in K) for T_o=20 °C. The solution for ΔT=0 corresponds to the one-parameter problem with constant fluid properties and apply for any $T_w \neq T_o$.

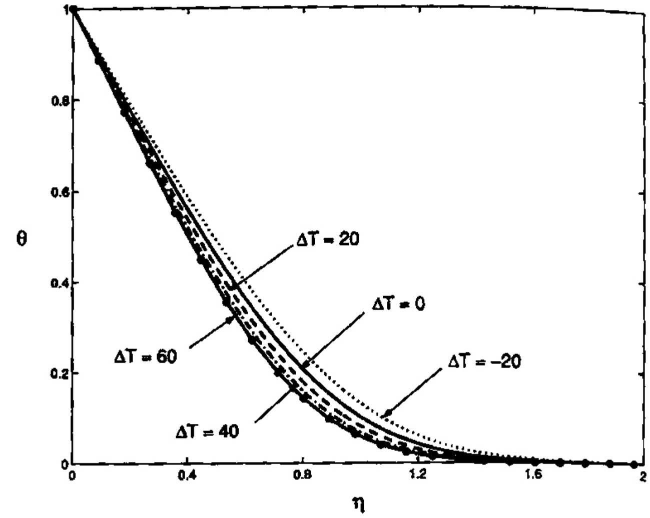

FIG. 4. Characteristic temperature profiles $\Theta(\eta)$ for some different ΔT (in K) for T_o=20 °C. The solution for ΔT=0 corresponds to the one-parameter problem with constant fluid properties and apply for any $T_w \neq T_o$.

V. RESULTS AND DISCUSSION

In the present context, the empirical correlations (14)–(16) are recast in terms of the dimensionless temperature $\Theta(\eta)$ defined in Eq. (10). The temperature T in Eqs. (14)–(16) is therefore taken as $T=T_0+\Delta T\Theta(\eta)$, where $\Delta T \equiv \lambda(T_w-T_0)$. Here, λ is a dimensionless parameter equal to unity, except in the special case of temperature-independent fluid properties for which $\lambda=0$. In general, however, the property relations take the form

$$\rho=\rho(\Theta;T_0,\Delta T); \quad \mu=\mu(\Theta;T_0,\Delta T); \quad \kappa=\kappa(\Theta;T_0,\Delta T). \tag{17}$$

The boundary value problem is thus a three-parameter problem of which the solution depends on T_0 and ΔT, together with the Prandtl number of the incoming film Pr_0. Here, Pr_0 is uniquely related to the inflow temperature T_0. Let us now recall that the similarity transformation does not exist in the special case $T_w=T_o$, for which the trivial solution $T(x,y)=T_o$ is readily obtained. The particular parameter value ΔT=0 only arises if λ=0 and thus implies that constant fluid properties are assumed, i.e., $\rho=\rho_o$, $\mu=\mu_o$, and $\kappa=\kappa_o$. The solutions for ΔT=0 are therefore equivalent with the solution of the one-parameter problem in Pr_0 (Ref. 5) and the results are valid for any $T_w \neq T_o$.

Some characteristic similarity profiles for the velocity and temperature fields are shown in Figs. 3 and 4, respectively. The inflow temperature was taken as T_0=20 °C in all cases. This temperature corresponds to an inflow Prandtl number Pr_0=6.98.

Figure 3 shows that the velocity f' in the hydrodynamic boundary layer is substantially affected by the temperature. This is an indirect effect through the temperature-dependent viscosity μ in the diffusive term in Eq. (11). Since the viscosity decreases with T, the diffusive momentum transport is correspondingly reduced with the consequence that the thickness δ of the hydrodynamic boundary layer decreases with increasing ΔT. When the wall temperature is lower than that of the incoming film, i.e., $\Delta T<0$, the water adjacent to the wall is cooled. The viscosity is therefore locally increased and the boundary layer thickens as compared with the special case ΔT=0, in which constant fluid properties are assumed. The opposite situation occurs when the wall is heated, i.e., $\Delta T>0$.

At a first glance at the temperature profiles in Fig. 4, it is observed that the thickness δ_T of the thermal boundary layer is somewhat less than half of the hydrodynamic boundary layer thickness δ. This is in accordance with the traditional rule-of-thumb $\delta/\delta_T \approx \sqrt{\mathrm{Pr}}$. Moreover, also the thermal boundary layer shrinks with increasing ΔT, i.e., with enhanced supply of thermal energy from the wall. The observed thinning of the thermal boundary layer is contrary to the effect expected by the increasing thermal diffusivity κ in Eq. (12). That effect is therefore more than outweighed by the increase of f in the convective transport term in (12), which is brought about by the higher velocity f'.

Exactly the same qualitative features as those observed in Figs. 3 and 4 were found also for inflow temperature T_0=60 °C, which corresponds to an inflow Prandtl number Pr_0=2.96 (velocity and temperature profiles are therefore not presented herein). Results for the wall gradients of the velocity and temperature for both T_0=20 °C and T_0=60 °C are compared in Figs. 5 and 6, respectively. These important film characteristics determine the local skin-friction coefficient

$$C_f \equiv \frac{\tau_w}{\frac{1}{2}\rho_0 U^2} = \frac{\rho_w \mu_w}{\rho_0 \mu_0} \cdot 3^{1/2} \cdot \mathrm{Re}_x^{-1/2} \cdot f''(0) \tag{18}$$

and the local Nusselt number

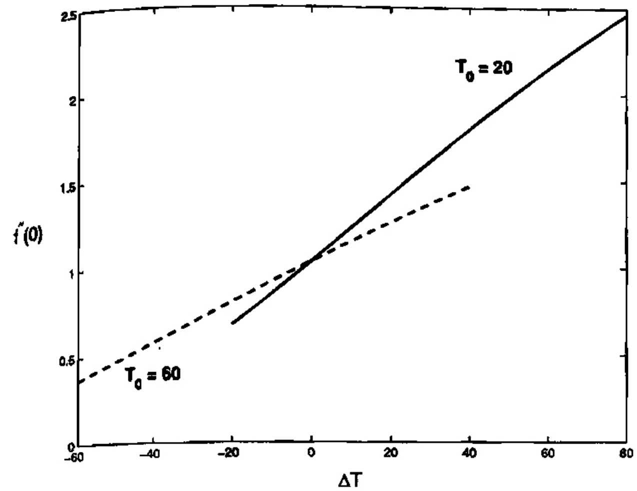

FIG. 5. Variation of the wall shear stress $f''(0)$ with ΔT (in K) for T_o=20 °C (solid line) and T_o=60 °C (broken line). The solution for ΔT=0 corresponds to the one-parameter problem with constant fluid properties and apply for any $T_w \neq T_o$.

$$\mathrm{Nu}_x \equiv -\frac{x}{T_w - T_0} \cdot \left.\frac{\partial T}{\partial y}\right|_w = -\frac{\rho_w}{\rho_0}\left(\frac{3}{4}\right)^{1/2} \cdot \mathrm{Re}_x^{1/2} \cdot \Theta'(0), \tag{19}$$

where $\mathrm{Re}_x \equiv U \cdot x/\nu_o$ is a local Reynolds number and $U=(2gx)^{1/2}$; cf. Eq. (2).

The wall gradient $f''(0)$ in Fig. 5 increases monotonically with the temperature difference ΔT in both cases, simply because of the thinning of the hydrodynamic boundary layer with increasing ΔT, cf. Fig. 3. The adjustment of the fluid velocity from no-slip ($f'=0$) at the wall to the free-stream velocity ($f'=1$) at the edge of the hydrodynamic boundary layer therefore takes place over a gradually narrower region δ. This thinning effect, which primarily stems from the temperature-dependent viscosity, is even more pronounced for T_0=20 °C than for T_0=60 °C. The nonlinear variation of μ in Eq. (15) is greater at the lower temperatures in the interval $T \in [0\ °\mathrm{C}, 100\ °\mathrm{C}]$, as seen from Fig. 2. The temperature dependency therefore plays the most important role at T_0=20 °C in Fig. 5. If instead of the nonlinear correlations (14)–(16) we had adopted linear or inversely linear temperature correlations, the results would be independent of the inflow temperature T_0. The particular parameter value ΔT=0 does not imply that $T_w = T_o$, but arises if $\lambda=0$ and thus makes the temperature dependency of ρ, μ, and κ vanish. The present problem then reduces to the film-flow problem with constant physical properties considered by Andersson[5] and $f''(0)$ becomes equal to 1.03890 just as in Ref. 5.

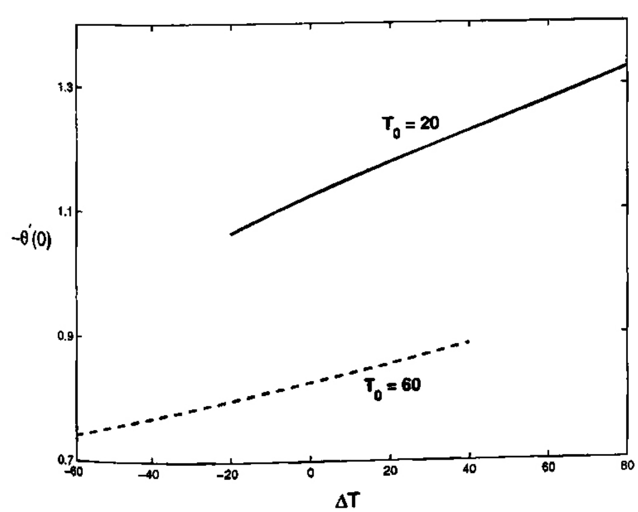

FIG. 6. Variation of the heat transfer rate $\Theta'(0)$ with ΔT (in K) for T_o=20 °C (solid line) and T_o=60 °C (broken line). The solution for ΔT=0 corresponds to the one-parameter problem with constant fluid properties and apply for any $T_w \neq T_o$.

The heat transfer rate at the wall is directly related to the temperature gradient $\Theta'(0)$ shown in Fig. 6. When the wall temperature exceeds the inflow temperature, i.e., $\Delta T > 0$, heat is transferred from the wall to the liquid film, whereas the heat transfer is reversed when $\Delta T < 0$. The magnitude of the dimensionless temperature gradient at the wall is a monotonically increasing function of the temperature difference ΔT both for T_0=20 °C and for T_0=60 °C. This is a consequence of the thinning of the thermal boundary layer with increasing temperature differences, as shown in Fig. 4. As suggested above, the thinning of the thermal boundary layer is directly associated with the thinning of the hydrodynamic boundary layer. This conjecture is consistent with the high Prandtl number asymptote

$$\mathrm{Nu}_x = \frac{3}{\Gamma(1/3)}\left(\frac{m+1}{2}\mathrm{Re}_x\right)^{1/2} \cdot \left(\frac{\mathrm{Pr}\, f''(0)}{3!}\right)^{1/3} \tag{20}$$

derived by Evans[11] for the Falkner-Skan-type of free-streams $U(x) \sim x^m$. Here, Γ denotes the gamma function and m is 1/2 according to Eq. (2). This high-Pr asymptote is valid also in the present case, provided that the temperature dependency is negligible for all physical properties but μ. The wall heat flux should therefore be proportional to $[f''(0)]^{1/3}$ in the limit as $\mathrm{Pr} \to \infty$.

It is evident that the Prandtl number $\mathrm{Pr} \equiv \mu C_p/\kappa$ varies with the temperature as a result of the temperature dependency of the physical properties, notably μ and κ. The effect of the variable Pr is, however, properly accounted for in the present analysis via the temperature-dependent μ in the momentum Eq. (11) and the temperature dependent κ in the thermal energy Eq. (12). It should therefore be emphasized that it is the Prandtl number Pr_0 of the incoming flow that enters into the transformed BVP (11)–(13). The substantially higher heat transfer rate for T_0=20 °C than for T_0=60 °C in Fig. 6 is simply due to the lower Pr_0 in the latter case.

The validity of the new similarity transformation relies on two rather different assumptions: (i) the range of applicability is restricted to the initial part of the film such that the boundary conditions (13b) can be justified; and (ii) the outer part of the film must exhibit a velocity variation consistent with Eq. (2). These assumptions will now be addressed separately.

The range of validity is based on the existence of an inviscid free stream between the momentum boundary layer and the surrounding quiescent atmosphere. This is no longer the case when the total volumetric film flow rate Q is confined within the momentum boundary layer. For a film with constant fluid properties, Andersson and Ytrehus[12] showed that the external free stream vanishes at

$$x^* = 0.1972 h_\infty \cdot Q/\nu, \tag{21}$$

where

$$h_\infty = (3\nu Q/g)^{1/3} \tag{22}$$

is the asymptotic limit of the film thickness $h(x)$ attained downstream of the acceleration zone where the film becomes fully developed; see, e.g., Alekseenko *et al.*[13] The actual numerical value in the above expression will obviously be somewhat affected by the presence of variable fluid properties, but the above relationship suffices for the present purpose. A further restriction might be that an isothermal layer with temperature T_a should be present outside the thermal boundary layer. For Prandtl numbers above unity, however, the thermal boundary layer is thinner than the momentum boundary layer. The similarity transformation (8)–(10) and the accompanying results there off are then valid within the streamwise range $0 < x < x^*$.

The distance x^*, for which the present approach is applicable, accordingly depends on the flow rate Q and kinematic viscosity ν. Lynn[14] carried out some experiments with a mixture of about 50% glycerine in water with kinematic viscosity $\nu \approx 6 \cdot 10^{-6}$ m^2 s^{-1}. For his highest film Reynolds number $Q/\nu \approx 200$ and asymptotic film thickness $h_\infty \approx 2.79$ mm, the extension of the zone of validity becomes $x^* \approx 110$ mm.

The second assumption, on which the present approach is based on, is the power-law variation of the free-stream velocity $U(x)$ in Eq. (2). This may be considered as a special case of the more general variation

$$U(x) = (U_{\text{in}}^2 + 2gx)^{1/2} \tag{23}$$

considered by Bruley[15] where U_{in} denotes the uniform inflow velocity at $x=0$. This more general variation of $U(x)$ does not permit similarity solutions of the boundary layer problem and Bruley therefore solved the governing boundary layer equation (4) as a partial differential equation (with constant fluid properties). Somewhat later, Cerro and Whitaker[16] and Yilmaz and Brauer[17] integrated the governing partial differential equations by means of a finite-difference approach. They observed an extremely fast rearranging of the surface position very close to the inlet when the initial film thickness was significantly larger than h_∞. In the present case, however, U_{in} is assumed negligible in order to allow for exact similarity to be achieved. This implies zero velocity U and infinite film thickness h at the inlet $x=0$. In view of the finite-difference solutions by Cerro and Whitaker[16] and Yilmaz and Brauer,[17] however, the film rapidly adjusts itself over a practically negligible distance. The infinite initial thickness is therefore of no practical concern.

VI. CONCLUDING REMARKS

A new similarity transformation (8)–(10) has been devised to enable a thorough investigation of the influence of variable physical properties on a gravity-driven liquid film flow along a vertical wall. The temperature-dependency of the fluid density prohibited the use of a Falkner-Skan-type transformation. The adopted Howarth-Dorodnitsyn-type transformation is applicable to general situations where the variation of all fluid properties is essential.

Sample calculations using nonlinear empirical correlations for water have been presented. Here, the temperature variation of the dynamic viscosity turns out to play a crucial role, not only directly in the momentum boundary layer but also indirectly in the thermal boundary layer. In fact, the reduction in viscosity due to a heated wall tends to accelerate the liquid film and thereby indirectly make the thermal boundary layer thinner. This observation conflicts with an anticipated thickening of the thermal boundary layer due to the enhanced thermal conductivity.

[1] K. D. Voskresensky, "Calculation of heat transfer in film condensation allowing for the temperature dependence of the physical properties of the condensate" (in Russian) Izv. Akad. Nauk SSSR, Otd. Tekh. Nauk, 1023 (1948).

[2] G. Poots and R. G. Miles, "Effects of variable physical properties on laminar film condensation of saturated steam on a vertical flat plate," Int. J. Heat Mass Transfer **10**, 1677 (1967).

[3] D.-Y. Shang and B.-X. Wang, "An extended study on steady-state laminar film condensation of a superheated vapour on an isothermal vertical plate," Int. J. Heat Mass Transfer **40**, 931 (1997).

[4] D.-Y. Shang, B.-X. Wang, Y. Wang, and Y. Quan, "Study on liquid laminar free convection with consideration of variable thermophysical properties," Int. J. Heat Mass Transfer **36**, 3411 (1993).

[5] H. I. Andersson, "Diffusion from a vertical wall into an accelerating falling liquid film," Int. J. Heat Mass Transfer **30**, 683 (1987).

[6] H. I. Andersson, B. A. Pettersson, and B. S. Dandapat, "Combined forced and natural convection in laminar film flow," Wärme- und Stoffübertrag. **29**, 399 (1994).

[7] V. M. Falkner and S. W. Skan, "Some approximate solutions of the boundary layer equations," Philos. Mag. **12**, 865 (1931).

[8] S. Schreier, *Compressible Flow* (Wiley, New York, 1982).

[9] *VDI-Wärmeatlas, Berechnungsblätter für den Wärmeübertragung* (5th Edition, VDI Verlage GmbH, Düsseldorf, 1988).

[10] J. Q. Chang, *Real Fluid Mechanics* (Tsinghua University Press, Beijing, 1986).

[11] H. L. Evans, *Laminar Boundary-Layer Theory* (Addison-Wesley, Reading, 1968).

[12] H. I. Andersson and T. Ytrehus, "Falkner-Skan solution for gravity-driven film flow," ASME J. Appl. Mech. **52**, 783 (1985).

[13] S. V. Alekseenko, V. E. Nakoryakov, and B. G. Pokusaev, *Wave Flow of Liquid Films* (Begell House, New York, 1994).

[14] S. Lynn, "The acceleration of the surface of a falling film," AIChE J. **6**, 703 (1960).

[15] D. F. Bruley, "Predicting vertical film flow characteristics in the entrance region," AIChE J. **11**, 945 (1965).

[16] R. L. Cerro and S. Whitaker, "Entrance region flows with a free surface: the falling liquid film," Chem. Eng. Sci. **26**, 785 (1971).

[17] T. Yilmaz and H. Brauer, "Beschleunigte Strömung von Flüssigkeitsfilmen an ebenen Wänden und in Füllkörperschichten," Chem.-Ing.-Tech. **45**, 928 (1973).